

Scalable Bayesian dynamic covariance modeling with variational Wishart and inverse Wishart processes

Creighton Heaukulani*

Mark van der Wilk[†]

Abstract

We implement gradient-based variational inference routines for Wishart and inverse Wishart processes, which we apply as Bayesian models for the dynamic, heteroskedastic covariance matrix of a multivariate time series. The Wishart and inverse Wishart processes are constructed from i.i.d. Gaussian processes, for which we apply existing black-box variational inference algorithms for approximate Gaussian process inference. These methods scale well with the length of the time series, however, they fail in the case of the Wishart process, an issue we resolve with a simple modification into an additive white noise parameterization of the model. This modification is also key to implementing a factored variant of the construction, allowing inference to additionally scale to high-dimensional covariance matrices. As with existing MCMC-based inference routines for the Wishart and inverse Wishart processes, we show that these variational alternatives significantly outperform multivariate GARCH baselines when forecasting the covariances of returns on financial instruments.

*Unaffiliated. Email: c.k.heaukulani@gmail.com.

[†]PROWLER.io, Cambridge, United Kingdom. Email: mark@proowler.io.

1 Introduction

Estimating the (time series of) covariance matrices between the variables in a multivariate time series is a principal problem of interest in many domains, particularly in finance and econometrics. Attaining good estimates of the entries of the covariance matrix presents a challenging problem, however, because there are $O(ND^2)$ parameters to estimate for a time series of length N with D variables, yet there are only $O(ND)$ observed data points. Bayesian models (and their corresponding inference procedures) often perform well in these overparameterized problems; indeed, Fox and West [7], Wilson and Ghahramani [20] and Fox and Dunson [6] show that Bayesian approaches based on the *Wishart* and *inverse Wishart processes* produce better estimates of dynamic covariance matrices than the venerable multivariate GARCH approaches [4, 5].

The Wishart and inverse Wishart processes are two related stochastic processes in the state space of symmetric, positive definite matrices, making them appropriate models for (heteroskedastic) time series of covariance matrices. They are themselves constructed from i.i.d. Gaussian processes, in analogy to the construction of Wishart or inverse Wishart random variables from i.i.d. Gaussian random variables. Previous authors have suggested inference routines for these models based on Markov chain Monte Carlo (MCMC) algorithms, which require exact posterior inference to be performed on the underlying Gaussian processes. We will instead rely on gradient-based variational inference routines for (sparse approximations of) the Gaussian process. This approach scales to large numbers of measurements N and has a simple, “black-box” implementation. We additionally derive a *factored* variant of the model that additionally scales inference to large numbers of variables D (i.e., to high dimensional covariance matrices). In our experiments, we will see that, like existing MCMC-based approaches to inference, our scalable, black-box, gradient-based, variational inference routines have predictive performance that dominates multivariate GARCH.

We start by considering variational inference routines for the model presented by Wilson and Ghahramani [20]; our approach is a gradient-based analogue of the coordinate ascent algorithms for variational inference on Wishart processes presented by van der Wilk et al. [19]. The factored variants of the model that we build toward in [Section 5](#) end up being a reparameterization of the construction by Fox and Dunson [6], and so our work provides gradient-based variational inference routines for their model class as well. Alternatively, Fox and West [7] construct inverse Wishart processes that are autoregressive (as opposed to the full process dependence assumed by the Gaussian processes); Wu et al. [22] model time series of (univariate) variances with Gaussian process models; and Wu et al. [21] consider generalizing multivariate GARCH by modeling the transition matrices of the process with autoregressive structures. All of these references elect MCMC-based inference and emphasize that Bayesian inference of (co)variances dominate non-Bayesian approaches.

2 Wishart and inverse Wishart processes

Let $Y := (Y_n, n \geq 1)$ denote a sequence of measurements in \mathbb{R}^D , which will be regressed upon a corresponding sequence of input locations (i.e., *covariates*) in \mathbb{R}^p denoted by $X := (X_n, n \geq 1)$. In our applications, we will take X_n to be a univariate (so $p = 1$), real-valued representation of the “time” at which the measurement Y_n was taken, and our goal is to model the time

series of covariances of Y . For example, in a dataset of daily stock returns, the vector Y_n can record the returns for D stocks on day n , for $n \leq N$, where the points in X can be linearly spaced in some fixed interval like $(0, 1)$ or $(-1, 1)$, and individual points of X may be altered to account for irregular spaces between some measurements, such as weekends or the removal of special trading days.

We let the conditional likelihood of Y_n be given by the mean zero multivariate Gaussian density

$$Y_n \mid \Sigma_n \sim \mathcal{N}(0, \Sigma_n), \quad n \geq 1, \quad (1)$$

for some sequence $\Sigma_1, \Sigma_2, \dots$ of (random) positive definite matrices, which we note depend on X . Bayesian models for Σ include the Wishart and inverse Wishart processes. In analogy to the construction of Wishart and inverse Wishart random variables from i.i.d. collections of Gaussian random variables, we may construct Wishart and inverse Wishart processes from i.i.d. collections of Gaussian processes as follows. Let

$$f_{d,k} \sim \text{GP}(0, \kappa(\cdot, \cdot; \theta)), \quad d \leq D, k \leq \nu, \quad (2)$$

be i.i.d. Gaussian processes with zero mean function and (shared) kernel function $\kappa(\cdot, \cdot; \theta)$, where θ denotes any parameters of the kernel function, and the positive integer-valued $\nu \geq D$ will be called the *degrees of freedom* parameter. Let $F_{n,d,k} := f_{d,k}(X_n)$, and for every $n \geq 1$, let $F_n := (F_{n,d,k}, d \leq D, k \leq \nu)$ denote the $D \times \nu$ matrix of collected function values. Construct

$$\Sigma_n = AF_n F_n^T A^T, \quad n \geq 1, \quad (3)$$

where $A \in \mathbb{R}^{D \times D}$ satisfies the condition that the symmetric matrix AA^T is positive definite.¹ So constructed, Σ_n is (marginally) Wishart distributed, and $\Sigma := (\Sigma_1, \Sigma_2, \dots)$ is correspondingly called a *Wishart process with degrees of freedom ν and scale matrix AA^T* . Alternatively, if we instead construct the precision matrix

$$\Sigma_n^{-1} = AF_n F_n^T A^T, \quad n \geq 1, \quad (4)$$

then Σ_n is inverse Wishart distributed, and Σ is called an *inverse Wishart process (with degrees of freedom ν and scale matrix AA^T)*. The dynamics of the process of covariance matrices Σ are inherited by the Gaussian processes, which are perhaps best controlled by the kernel function $\kappa(\cdot, \cdot; \theta)$.

The sequence of Gaussian likelihoods in [Eq. \(1\)](#) is conjugate to the law of the inverse Wishart process, upon which existing MCMC-based approaches to inference typically rely. In contrast, the “black-box” variational inference routines that we suggest only require evaluations of the log conditional likelihood function, dramatically simplifying their implementation. For the Wishart process case, we have

$$\log p(Y_n \mid F_n) = -\frac{D}{2} \log(2\pi) - \frac{1}{2} \log |AF_n F_n^T A^T| - \frac{1}{2} Y_n^T (AF_n F_n^T A^T)^{-1} Y_n, \quad (5)$$

and for the inverse Wishart case, we have

$$\log p(Y_n \mid F_n) = -\frac{D}{2} \log(2\pi) + \frac{1}{2} \log |AF_n F_n^T A^T| - \frac{1}{2} Y_n^T AF_n F_n^T A^T Y_n. \quad (6)$$

¹Alternatively, we may take A to be the (triangular) cholesky factor of a positive definite matrix AA^T .

3 Sparse Gaussian process approximations and variational inference

Existing MCMC-based inference routines for the Wishart and inverse Wishart processes rely on exact posterior inference for the underlying Gaussian processes, requiring computations dominated by $O(N^3)$ matrix inversions and having memory requirements dominated by the storage of the $O(N^2)$ covariance matrix. A standard approach to reduce this complexity employs a sparse approximation to the Gaussian process defined by a set of M *inducing points* $Z := (Z_1, \dots, Z_M)$, taking values in the same space as the inputs X , upon which we assume the dependence of the function values F_n decouple during inference [1, 9, 16]. In particular, for every $d \leq D$ and $k \leq \nu$, let $U_{m,d,k} := f_{d,k}(Z_m)$, $m \leq M$, denote the evaluations of the Gaussian process at the inducing points, and collectively denote $U_{d,k} := (U_{m,d,k}, m \leq M)$ and $F_{d,k} := (F_{n,d,k}, n \leq N)$. By independence, and with well-known properties of the Gaussian distribution, we may write

$$p(Y, F, U) = \prod_{n=1}^N [p(Y_n | F_n)] \prod_{d=1}^D \prod_{k=1}^{\nu} [p(F_{d,k} | U_{d,k}) p(U_{d,k})], \quad (7)$$

where $p(F_{d,k} | U_{d,k}) p(U_{d,k}) = \mathcal{N}(F_{d,k}; K_{xz} K_{zz}^{-1} U_{d,k}, K_{xx} - K_{xz} K_{zz}^{-1} K_{xz}^T) \mathcal{N}(U_{d,k}; 0, K_{zz})$, and where the $N \times N$ matrix K_{xx} has (n, n') -th element $\kappa(X_n, X_{n'}; \theta)$, the $N \times M$ matrix K_{xz} has (n, m) -th element $\kappa(X_n, Z_m; \theta)$, and the $M \times M$ matrix K_{zz} has (m, m') -th element $\kappa(Z_m, Z_{m'}; \theta)$.

Following Hensman et al. [10], we introduce a variational approximation to the posterior distribution of the latent variables that takes the following form: Independently for every $d \leq D$ and $k \leq \nu$, let $q(F_{d,k}, U_{d,k}) = p(F_{d,k} | U_{d,k}) q(U_{d,k})$, where $q(U_{d,k}) = \mathcal{N}(U_{d,k}; \mu_{d,k}, S_{d,k})$, for some *variational parameters* $\mu_{d,k} \in \mathbb{R}^M$ and $S_{d,k} \in \mathbb{R}^{M \times M}$ a real, symmetric, positive definite matrix. It follows that

$$q(F_{d,k}) = \int p(F_{d,k} | U_{d,k}) q(U_{d,k}) dU_{d,k} = \mathcal{N}(F_{d,k}; \tilde{K} \mu_{d,k}, K_{xx} + \tilde{K} (S_{d,k} - K_{zz}) \tilde{K}^T), \quad (8)$$

where $\tilde{K} := K_{xz} K_{zz}^{-1}$. That is, the variational approximation $q(U_{d,k})$ *induces* the approximation $q(F_{d,k})$, which can be extended to the full Gaussian process over the whole input domain [2]. We may then lower bound the log marginal likelihood of the data as follows:

$$\log p(Y) \geq \sum_{n=1}^N \mathbb{E}_{q(F_n)} [\log p(Y_n | F_n)] - \sum_{d=1}^D \sum_{k=1}^{\nu} \text{KL}[q(U_{d,k}) || p(U_{d,k})], \quad (9)$$

where $\text{KL}[q || p]$ denotes the Kullback–Leibler divergence. To perform inference, we maximize the *evidence lower bound* on the right hand side of Eq. (9)—which we note depends on the parameters to be optimized $\Theta := \{Z, \mu, S, \theta\}$ through the variational distribution q —via gradient ascent. This minimises the KL divergence between the approximate posterior process Eq. (8) and the true posterior process [2]. The terms $\text{KL}[q(U_{d,k}) || p(U_{d,k})]$ may be analytically evaluated and so their gradients (w.r.t. the optimization parameters) are straightforward to compute. Because $q(F)$ is not conjugate to the likelihood $p(Y | F)$, we cannot analytically evaluate the term $\mathbb{E}_{q(F_n)} [\log p(Y_n | F_n)]$. We therefore follow Salimans

and Knowles [17] and Kingma and Welling [12] to approximate the gradients of (Monte Carlo estimates of) this expression by “differentiating through” random samples from q as follows.

Independently for every $d \leq D$ and $k \leq \nu$, let $w_{d,k}^{(r)} \sim \mathcal{N}(0, I_N)$ be i.i.d. for $r = 1, \dots, R$. Set $F_{d,k}^{(r)} = \psi_{d,k}(w_{d,k}^{(r)}; \Theta)$, where $\psi_{d,k}(w; \Theta) := B_{d,k}w + \tilde{K}\mu_{d,k}$, for the matrix $B_{d,k} \in \mathbb{R}^{N \times N}$ that satisfies $B_{d,k}B_{d,k}^T = K_{xx} + \tilde{K}(S_{d,k} - K_{zz})\tilde{K}^T$, as given by the Cholesky factor. Note that $F_{d,k}^{(r)}$ has distribution $q(F_{d,k})$. This forms the Monte Carlo approximations

$$\nabla_{(\mu_{d,k}, S_{d,k})} \mathbb{E}_{q(F_n)} [\log p(Y_n | F_n)] \approx \frac{1}{R} \sum_{r=1}^R \left[\nabla_{F_{d,k}} \log p(Y_n | F_n^{(r)}) \circ \nabla_{(\mu_{d,k}, S_{d,k})} \psi_{d,k}(w_{d,k}^{(r)}; \Theta) \right],$$

for every $d \leq D$ and $k \leq \nu$, where \circ denotes the element-wise product, and

$$\nabla_{(Z, \theta)} \mathbb{E}_{q(F_n)} [\log p(Y_n | F_n)] \approx \frac{1}{R} \sum_{r=1}^R \sum_{d=1}^D \sum_{k=1}^{\nu} \left[\nabla_{F_{d,k}} \log p(Y_n | F_n^{(r)}) \circ \nabla_{(Z, \theta)} \psi_{d,k}(w_{d,k}^{(r)}; \Theta) \right].$$

These unbiased estimators often have low enough variance that a single Monte Carlo sample suffices for the approximation [17]. Finally, the gradients of the lower bound on the right hand side of Eq. (9) with respect to $\mu_{d,k}$ and $S_{d,k}$ may then be approximated by the unbiased estimator

$$\frac{N}{|\mathcal{B}|} \sum_{n \in \mathcal{B}} \left[\nabla_{(\mu_{d,k}, S_{d,k})} \mathbb{E}_{q(F_n)} [\log p(Y_n | F_n)] \right] - \nabla_{(\mu_{d,k}, S_{d,k})} \text{KL}[q(U_{d,k}) || p(U_{d,k})], \quad (10)$$

where $\mathcal{B} \subseteq \{(X_n, Y_n) : n \leq N\}$ is a minibatch of the datapoints. Likewise, the gradients with respect to Z and θ may be approximated by

$$\frac{N}{|\mathcal{B}|} \sum_{n \in \mathcal{B}} \left[\nabla_{(Z, \theta)} \mathbb{E}_{q(F_n)} [\log p(Y_n | F_n)] \right] - \sum_{d=1}^D \sum_{k=1}^{\nu} \nabla_{(Z, \theta)} \text{KL}[q(U_{d,k}) || p(U_{d,k})]. \quad (11)$$

With the gradient approximations in Eqs. (10) and (11), gradient ascent may now be carried out with a Robbins–Monro stochastic approximation routine.

Implementing this routine may be treated like a “black-box”, since switching between the Wishart and inverse Wishart processes only requires plugging in the appropriate log conditional likelihood function $\log p(Y_n | F_n)$, given by Eq. (5) or Eq. (6). For simplicity, assume $\nu = D$; producing a Monte Carlo sample from $q(F_{d,k})$ for the minibatch \mathcal{B} scales computationally in $O(N_b^3 + N_b M^2 + M^3)$, where $N_b := |\mathcal{B}|$, and has memory requirements in $O(N_b^2 + N_b M + M^2)$. Producing this for every $d \leq D$, $k \leq \nu$, together with the computation of $\log p(Y_n | F_n)$, results in an overall computational complexity in $O(N_b D^3 + D^2(N_b^3 + N_b M^2 + M^3))$ and memory requirement in $O(D^2(N_b^2 + N_b M + M^2))$. The inference procedure is implemented in GPflow [14], a Gaussian process toolbox built on Tensorflow.

4 The additive white noise model

In our initial experiments, we found that the inverse Wishart parameterization successfully moved the parameters into a good region of the state space, whereas the Wishart process

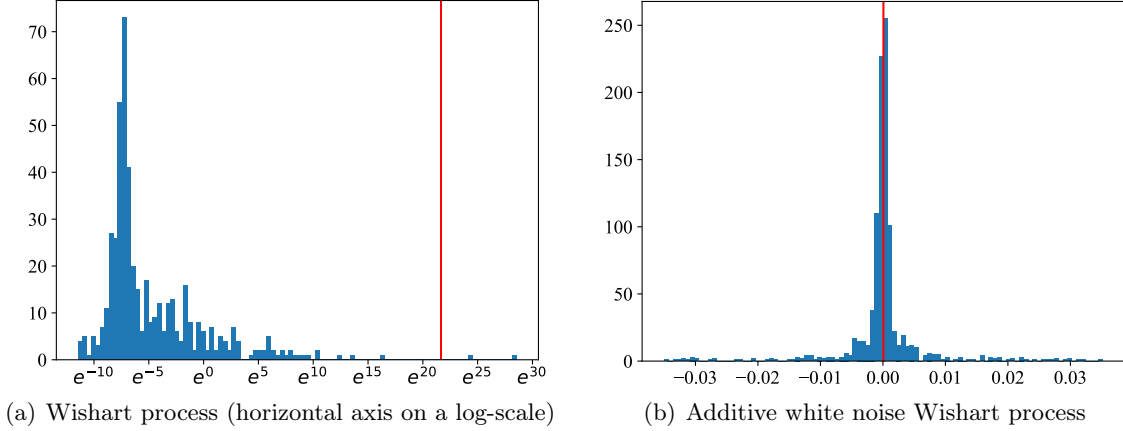


Figure 1: Histograms of 1,000 Monte Carlo samples of the gradient with respect to the variable $F_{1,1,1}$ in a univariate model. **Fig. 1(a)** shows an extremely skewed distribution in the case of the Wishart process, and **Fig. 1(b)** shows its correction under the additive white noise reparameterization. The mean of each distribution is shown as a red horizontal line.

failed to move the parameters in the correct direction (based on traceplots of parameters and validation metrics). It appears that this failure is due to extremely high variance of the Monte Carlo gradient approximation routine. By studying the log likelihood function for the Wishart process in [Eq. \(5\)](#), we hypothesize that evaluating the inverse in the final term, $-\frac{1}{2}Y_n^T(AF_nF_n^TA^T)^{-1}Y_n$, on Monte Carlo samples of F_n (which is required by the black-box variational inference procedure) is problematic because those samples can often be close to the origin, resulting in this quantity being extremely large in magnitude. For example, in the case of a univariate output, i.e., $D = 1$, and corresponding unit scale $A = 1$, the likelihood involves computation of the scalar term $-\frac{1}{2}y_n^2/f_n^2$, which is large in magnitude for samples when f_n is closer to zero than the data point y_n , a problem that is exacerbated by the quadratic scales.

To visualize this issue, consider a bivariate output Y_n with constant covariance matrix $\Sigma_n = [[2.0, 1.9], [1.9, 2.0]]$ and $A = [[1, 0], [0, 1]]$. We let $\nu = D = 2$ and simulated a dataset Y_n for $n \leq 30$ at input locations X_n , which together with some inducing points Z_m , $m \leq 10$, are sampled uniformly in $(0, 1)$. Following the procedure in [Section 3](#), we compute 1,000 samples of

$$\nabla_{F_{d,k}} \log p(Y_n | F_n^{(r)}), \quad F_{d,k}^{(r)} \sim q(F_{d,k}), \quad d \leq 2, k \leq 2, n \leq 30, r \leq 1000, \quad (12)$$

and display a histogram of the samples corresponding to the variable $F_{1,1,1}$ in **Fig. 1(a)**, where the horizontal axis is on a *log scale*. The distribution is extremely skewed; the mean of these samples, at around 2.5×10^9 , is plotted as a red vertical line, and the standard deviation is 7.9×10^{10} !

To resolve this issue, consider once again the case when $D = 1$ with unit scale $A = 1$. We can modify the previously problematic scalar term to be $-\frac{1}{2}y_n^2/(f_n^2 + \lambda)$, where the denominator is shifted away from zero by a parameter $\lambda > 0$. More generally, we can accomplish this with a slightly generalized construction to that studied by van der Wilk et al.

[19]: Construct the covariance matrix of y_n as

$$\Sigma_n := AF_n F_n^T A^T + \Lambda, \quad n \geq 1, \quad (13)$$

where Λ is a diagonal $D \times D$ matrix with positive (diagonal) entries. To interpret this modification, note that the model in [Section 2](#) may be alternatively written as $y_n = AF_n z_n$, where $z_n \sim \mathcal{N}(0, I_\nu)$, for $n \geq 1$, so that $\text{cov}(y_n | F_n) = AF_n F_n^T A^T$. The modified construction may be instead written as

$$y_n = AF_n z_n + \varepsilon_n, \quad z_n \sim \mathcal{N}(0, I_\nu), \quad \varepsilon_n \sim \mathcal{N}(0, \Lambda), \quad n \geq 1, \quad (14)$$

and so $\text{cov}(y_n | F_n) = AF_n F_n^T A^T + \Lambda$. This modification may therefore be interpreted as introducing *white* (or *observational*) noise to the model. The log likelihood in [Eq. \(5\)](#) is replaced by

$$\log p(Y_n | F_n) = \frac{ND}{2} \log(2\pi) - \log |AF_n F_n^T A^T + \Lambda| - \frac{1}{2} Y_n^T (AF_n F_n^T A^T + \Lambda)^{-1} Y_n. \quad (15)$$

The approximated gradients may now be stably computed: In [Fig. 1\(b\)](#), we plot a histogram of the samples of the gradients in [Eq. \(12\)](#) for this modified model, where $\Lambda = [[0.01, 0.0], [0.0, 0.01]]$.

While the inverse Wishart case does not suffer such computational issues, we will see in [Section 5](#) that this additive white noise modification is the key to a *factored* variant of both the Wishart and inverse Wishart processes, inference for which is tractable for high-dimensional covariance matrices. In the inverse Wishart case, however, a useful additive white noise modification is not easy to implement. We consider instead the following construction for the precision matrix

$$\Sigma_n^{-1} := AF_n F_n^T A^T + \Lambda^{-1}, \quad n \geq 1, \quad (16)$$

where, as a diagonal matrix, Λ^{-1} contains the inverted elements on the diagonal of Λ . If the variables in y_n are independent, then the elements of Λ retain their interpretation as (the variances of) additive white noise. More generally, they have an interpretation as additive terms to the *partial variances* of the variables in y_n . The log likelihood in [Eq. \(6\)](#) is now replaced by

$$\log p(Y_n | F_n) = \frac{ND}{2} \log(2\pi) + \log |AF_n F_n^T A^T + \Lambda^{-1}| - \frac{1}{2} Y_n^T (AF_n F_n^T A^T + \Lambda^{-1}) Y_n. \quad (17)$$

In our experiments, we infer the parameters of Λ with maximum likelihood.

5 Factored covariance models

The computational and memory requirements of inference in the models so far presented scale with D in $O(D^3)$ and $O(D^2)$, respectively, since we must invert (or take the determinant of) the $D \times D$ covariance or precision matrix. This will become intractable for even moderate values of D , which is particularly troublesome in applications like finance where D could, for example, represent the number of financial instruments in a large stock market index

like the S&P 500. To reduce this complexity, consider fixing some $K \ll D$ and reducing F_n to be of size $K \times \nu$, for some $\nu \geq K$. The matrix $F_n F_n^T$ is a $K \times K$ Wishart-distributed matrix. Let A now be of size $D \times K$. Then by the properties of the Wishart distribution, the $D \times D$ matrix $A F_n F_n^T A^T$ is also Wishart-distributed. This factor-like, low-rank model has significantly fewer parameters than those in [Sections 2 and 4](#).

Consider applying this construction to the additive white noise model for the Wishart process described in [Section 4](#), where $\Sigma_n = A F_n F_n^T A^T + \Lambda$. Recalling that Λ is diagonal, the log likelihood function in [Eq. \(15\)](#) may be computed efficiently with the Woodbury matrix identities as follows:

$$\begin{aligned} \log p(Y_n | F_n) = & \frac{ND}{2} \log(2\pi) - \frac{1}{2} \sum_{d=1}^D \log \Lambda_{d,d} + \frac{1}{2} \log |I_\nu + F_n^T A^T \Lambda^{-1} A F_n| \\ & - \frac{1}{2} Y_n^T \Lambda^{-1} Y_n + \frac{1}{2} Y_n^T A F_n (I_\nu + F_n^T A^T \Lambda^{-1} A F_n)^{-1} F_n^T A^T Y_n. \end{aligned} \quad (18)$$

In the inverse Wishart case, we have $\Sigma_n^{-1} = A F_n F_n^T A^T + \Lambda^{-1}$, which we note is a reparameterization of the construction by Fox and Dunson [\[6\]](#). The log likelihood function in this case is

$$\begin{aligned} \log p(Y_n | F_n) = & \frac{ND}{2} \log(2\pi) + \frac{1}{2} \sum_{d=1}^D \log \Lambda_{d,d} - \frac{1}{2} \log |I_\nu + F_n^T A^T \Lambda A F_n| \\ & - \frac{1}{2} Y_n^T \Lambda^{-1} Y_n - \frac{1}{2} Y_n^T A F_n F_n^T A^T Y_n. \end{aligned} \quad (19)$$

For simplicity, assume $\nu = K$. Then these log likelihood functions may be computed in $O(DK^2)$ time and $O(DK)$ space. With the black-box approach to variational inference, we need only drop the likelihood expressions in [Eqs. \(18\) and \(19\)](#) into the gradient approximations in [Eqs. \(10\) and \(11\)](#). The overall complexity then reduces to computations in $O(N_b DK^2 + K^2(N_b^3 + N_b M^2 + M^3))$ and memory requirements in $O(DK + K^2(N_b^2 + N_b M + M^2))$. This model and inference procedure is therefore scalable to both large N and D regimes.

6 Experiments on financial returns

We implement our variational inference routines on variants of the models applied to several datasets of financial returns. The datasets are denoted as follows (note that we take the *log returns*, which are defined at time $t + 1$ is as $\log(1 + P_{t+1}/P_t)$, where P_t is the price of the instrument at time t):

Dow 30: Intraday returns on the components of the Dow 30 Industrial Average (as of the changes on Jun. 8, 2009), taken at the close of every five-minute interval from Nov. 17, 2017 through Dec. 6, 2017. The resulting dataset size is $N = 978$, $D = 30$. The raw data was from Marjanovic [\[13\]](#).

FX: Daily foreign exchange rates for 20 currency pairs taken from Wu et al. [\[22\]](#). The dataset size is $N = 1,565$, $D = 20$.

S&P 500: Daily returns on the closing prices of the components of the S&P 500 index between Feb. 8, 2013 through Feb. 7, 2018, taken from Nugent [\[15\]](#). Missing prices are

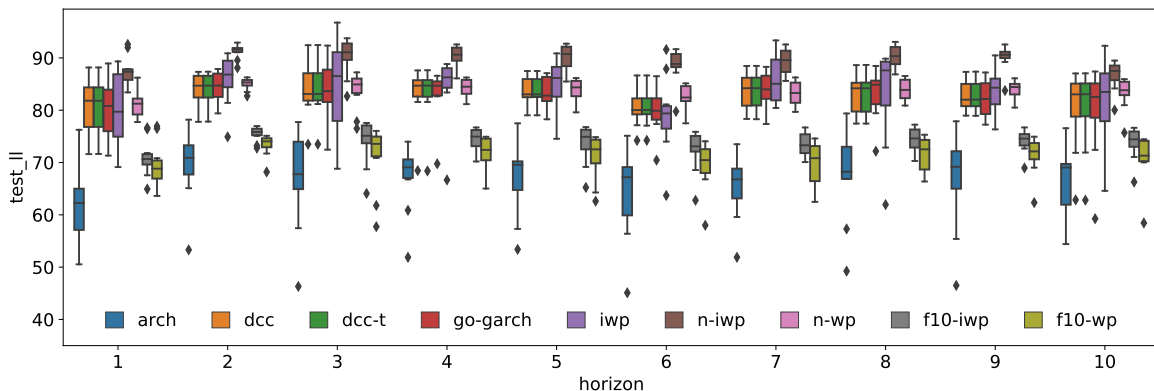


Figure 2: Example display of the results for the FX dataset. A set of boxplots reporting the test loglikelihoods of the predictions is displayed for each step of the 10-step forecast horizon (indicated on the horizontal axis). Each boxplot contains the scores from the 10 training/testing splits.

forward-filled. The resulting dataset size is $N = 1,258$, $D = 505$ (there are 505 names in the index).

The simplest baseline is univariate ARCH (applied to each variable independently), implemented through the Python package `arch` [18]. The MGARCH variants we compare to are the *dynamic conditional correlation* model (DCC) [4] with Gaussian and multivariate-t emission distributions, and the *generalized orthogonal garch* model (GO-GARCH) [3], a competitive variant of the BEKK MGARCH specification. These baselines are among the dominant MGARCH modeling approaches and were implemented through the R package `rmgarch` [8]. The MGARCH baselines do not scale to the S&P 500 dataset, and there are no ubiquitous baselines in this large covariance regime.

For each dataset, we created 10 evenly-sized training and testing sets with a rolling window, where the test set comprises 10 consecutive measurements following the training set (we may therefore consider a 10-step-ahead forecasting task), and no testing sets overlap. To evaluate the models, we take the 10-step-ahead forecast of the covariance matrix, say, Σ_t^* at test time t , and compute the log-likelihood of the corresponding test set Y_t under a mean-zero Gaussian distribution with covariance Σ_t^* . In order to easily understand this setup, we display the results for just one experiment in Fig. 2 as a series of grouped histograms. The horizontal axis represents the forecast horizon; at each horizon, the boxplot of test-loglikelihoods (over the 10 training/testing sets) are displayed for each model. The two core modeling paradigms are denoted as ‘wp’ and ‘iwp’ for the Wishart and inverse Wishart process variants, respectively. If the additive white noise variant described in Section 4 is used (with a non-factored covariance model), we prepend the model name with ‘n-’. The factored model variants, described in Section 5, have model names prepended with ‘f[K]-’, where [K] is the number of factors. We used a GP covariance kernel composed as the sum of a Matern 3/2 kernel, a rational quadratic kernel and a periodic component, which is itself composed as the product of a periodic kernel and radial basis function kernel. The ARCH baseline is denoted ‘arch’, the DCC baselines with a multivariate normal and multivariate-t likelihood are denoted ‘dcc’ and ‘dcc-t’, respectively, and the GO-GARCH baseline is denoted

‘go-garch’.

Further details for our experimental setup are as follows: We used a diagonal matrix A for the full-rank (non-factored) covariance models. The parameters in A and Λ are inferred by maximum likelihood. The values of Λ were initialized to $\Lambda_{d,d} = 0.001$, $d \leq D$. The degrees of freedom parameter ν is set to the number of variables D , or the number of factors K in the factored covariance cases. We did not find performance to be sensitive to this choice. We used $M = 300$ inducing points, $R = 2$ variational samples for the Monte Carlo approximations, and a minibatch size of 300. The gradient ascent step sizes were scheduled according to Adam [11]. We selected the stopping times (and in some cases, a learning rate decay schedule) via cross validation, choosing the setting that maximized the total test loglikelihood metric (see below) on a validation set. The validation sets were the final 2%, 5%, and 5% of the measurements in a randomly selected training set for the Dow 30, FX, and S&P 500 datasets, respectively.

We consider three different metrics: A *total* prediction score that sums the log-likelihoods across the 10-step forecast horizon; a *one-step ahead* prediction score; and a *10-step ahead* prediction score. The results for these three tasks are displayed in Tables 1 to 3, respectively. We report the mean score \pm one standard deviation across the 10 training/testing windows. The highest score for each dataset is bolded. We also provide, in brackets, the p-value of a paired t-test between the scores of each model and the highest performing MGARCH baseline (for the task and dataset, which was always either go-garch or dcc-t), highlighting with a * when significant at a 0.05 level.

One of either the Wishart or inverse Wishart process variants dominates the performance of MGARCH in all cases, as was found with MCMC approaches to inference. We may conclude that taking the variational approach to inference has not lost this competitive performance. Of the MGARCH baselines, either go-garch or dcc-t performed best in each case. Note that the additive white noise variant of the inverse Wishart process outperforms the standard variant (‘n-iwp-p’ vs. ‘iwp-p’), which is measured significant (p-values of 5.42e-3 and 3.42e-2 for the Dow 30 and FX datasets, respectively) and can perhaps be explained by the extra flexibility afforded by the additional parameters for the additive white noise model. Interestingly, the inverse Wishart process variants always seem to outperform their Wishart process counterparts. This may be partially explained by the avoidance of one cholesky factorization in the computation of the log-likelihood functions for the inverse Wishart case, given by Eqs. (6) and (19), improving numerical accuracy both during inference and when evaluating the test metrics. At the very least, we can suggest at this point that the inverse Wishart processes should be given preference by practitioners. On the Dow 30 and FX datasets, the factored variants always underperformed MGARCH, confirming that when one is able to employ a full-rank covariance model, they should. In the case of the S&P 500 dataset, the full-rank covariance models and the MGARCH baselines may not be feasible. The factored covariance models outperform the ARCH baseline, and increasing the number of factors from $K = 10$ to $K = 30$ results in a significant improvement (p-value is 9.58e-3 for ‘f10-wp’/‘f30-wp’ and 1.08e-2 for ‘f10-iwp’/‘f30-iwp’). Finally, when analyzing the performance at different forecasting horizons, the performance at the one-step horizon often looks similar to the total performance metric. However, at the further 10-step horizon, the performance of the MGARCH baselines degrade, which can be seen for example by noting that their scores often drop below the factored covariance models. We may conclude that the

Table 1: Total test loglikelihood metric over the 10-step forecast horizon. The displayed metric is the mean score over the 10 train/test sets, along with \pm one std. dev. The highest score is bolded. The p-values for a paired t-test comparing each set of scores with the best performing MGARCH baseline are also shown in brackets, highlighted with a * if significant at a 0.05 level.

	Dow 30	FX	S&P 500
arch	1422.32 \pm 98.35	664.90 \pm 48.78	13581.28 \pm 1983.69
dcc	1625.12 \pm 226.82	825.19 \pm 15.37	–
dcc-t	1627.62 \pm 224.85	825.33 \pm 15.51	–
go-garch	1643.80 \pm 243.05	823.55 \pm 15.40	–
iwp	1660.33 \pm 269.22* (2.11e-2)	837.13 \pm 5.82* (6.17e-3)	–
n-iwp	1663.01 \pm 269.99* (2.92e-3)	902.84 \pm 6.24* (1.44e-7)	–
n-wp	1647.33 \pm 253.38* (6.47e-3)	836.12 \pm 18.77* (5.97e-3)	–
f10-iwp	1630.03 \pm 215.34	738.76 \pm 8.68	14382.56 \pm 775.03
f10-wp	1618.44 \pm 184.17	707.58 \pm 9.87	13947.30 \pm 1211.26
f30-iwp	–	–	14393.27 \pm 787.11
f30-wp	–	–	13927.64 \pm 1244.45

Wishart and inverse Wishart processes are better at multi-step forecasting than MGARCH.

7 Conclusion

For small covariance dimensionality, a full-rank covariance model (unsurprisingly) performs best, and our results suggest that the additive white noise parameterization of the inverse Wishart process should be preferred. Selecting the desired modeling variant is easy, since the black-box approach to variational inference is rather straightforward to implement, especially with tools like GPflow. However, we hope the failure of these techniques in the case of the Wishart process provides a warning to practitioners that these methods cannot be always be trusted as black-boxes in all cases.

References

- [1] M. Bauer, M. van der Wilk, and C. E. Rasmussen. Understanding probabilistic sparse Gaussian process approximations. In *NIPS*, 2016.
- [2] A. G. de G. Matthews, J. Hensman, R. Turner, and Z. Ghahramani. On sparse variational methods and the Kullback–Leibler divergence between stochastic processes. In *AISTATS*, 2016.
- [3] R. Van der Weide. GO-GARCH: a multivariate generalized orthogonal GARCH model. *Journal of Applied Econometrics*, 17(5):549–564, 2002.
- [4] R. Engle. Dynamic conditional correlation: A simple class of multivariate generalized autoregressive conditional heteroskedasticity models. *Journal of Business & Economic Statistics*, 20(3):339–350, 2002.

Table 2: One-step-ahead test loglikelihood metric. See the caption of Table 1 for details.

	Dow 30	FX	S&P 500
arch	143.22 ± 10.12	62.13 ± 7.00	1484.29 ± 123.50
dcc	172.48 ± 7.51	80.71 ± 4.94	–
dcc-t	172.60 ± 7.27	80.73 ± 4.94	–
go-garch	173.80 ± 6.92	79.85 ± 5.41	–
iwp	$179.98 \pm 8.38^* (4.91\text{e-}2)$	$80.37 \pm 2.88^* (6.14\text{e-}3)$	–
n-iwp	$182.70 \pm 7.67^* (1.90\text{e-}2)$	$87.17 \pm 6.71^* (1.42\text{e-}4)$	–
n-wp	$179.11 \pm 7.30 (6.94\text{e-}2)$	$81.40 \pm 2.73 (5.49\text{e-}2)$	–
f10-iwp	169.59 ± 7.27	70.90 ± 3.38	1392.59 ± 240.73
f10-wp	167.85 ± 4.89	67.44 ± 4.11	1388.94 ± 236.25
f30-iwp	–	–	1396.93 ± 242.09
f30-wp	–	–	1388.89 ± 236.06

Table 3: Ten-step-ahead test loglikelihood metric. See the caption of Table 1 for details.

	Dow 30	FX	S&P 500
arch	149.59 ± 5.22	66.58 ± 6.37	1422.26 ± 111.84
dcc	167.61 ± 6.22	80.28 ± 7.20	–
dcc-t	167.84 ± 5.93	80.30 ± 7.21	–
go-garch	171.29 ± 6.56	79.92 ± 8.11	–
iwp	$173.49 \pm 10.92^* (5.06\text{e-}3)$	$80.68 \pm 2.72^* (6.46\text{e-}3)$	–
n-iwp	$179.98 \pm 9.69^* (2.70\text{e-}2)$	$87.92 \pm 9.10^* (2.74\text{e-}3)$	–
n-wp	$175.30 \pm 7.01^* (5.59\text{e-}3)$	$83.24 \pm 2.92^* (8.28\text{e-}03)$	–
f10-iwp	169.80 ± 6.32	73.69 ± 2.98	1450.07 ± 106.42
f10-wp	168.12 ± 4.69	70.86 ± 4.48	1442.58 ± 106.38
f30-iwp	–	–	1452.74 ± 104.87
f30-wp	–	–	1442.23 ± 106.31

- [5] R. F. Engle and K. F. Kroner. Multivariate simultaneous generalized ARCH. *Econometric Theory*, 11(1):122–150, 1995.
- [6] E. B. Fox and D. B. Dunson. Bayesian nonparametric covariance regression. *Journal of Machine Learning Research*, 16:2501–2542, 2015.
- [7] E. B. Fox and M. West. Autoregressive models for variance matrices: Stationary inverse Wishart processes. *arXiv preprint arXiv:1107.5239*, 2011.
- [8] A. Ghalanos. rmgarch: Multivariate GARCH models, 2014. URL <https://cran.r-project.org/web/packages/rmgarch>. R package version 1.2-8.
- [9] J. Hensman, N. Fusi, and N. D. Lawrence. Gaussian processes for big data. In *UAI*, 2013.
- [10] J. Hensman, A. G. de G. Matthews, and Z. Ghahramani. Scalable variational Gaussian process classification. In *AISTATS*, 2015.
- [11] D. P. Kingma and J. Ba. Adam: a method for stochastic optimization. In *ICLR*, 2015.

- [12] D. P. Kingma and M. Welling. Auto-encoding variational Bayes. In *ICLR*, 2014.
- [13] Boris Marjanovic. Huge stock market dataset. Kaggle.com, Nov. 2017. URL <https://www.kaggle.com/borismarjanovic/price-volume-data-for-all-us-stocks-etfs>. Version 3. Last updated 11/10/2017.
- [14] A. G. de G. Matthews, M. van der Wilk, T. Nickson, K. Fujii, A. Boukouvalas, P. León-Villagrà, Z. Ghahramani, and J. Hensman. GPflow: A Gaussian process library using TensorFlow. *Journal of Machine Learning Research*, 18(40):1–6, 2017.
- [15] Cam Nugent. S&p 500 stock data. Kaggle.com, Feb. 2018. URL <https://www.kaggle.com/camnugent/sandp500>. Version 4.
- [16] J. Quiñonero-Candela and C. E. Rasmussen. A unifying view of sparse approximate Gaussian process regression. *Journal of Machine Learning Research*, 6:1939–1959, 2005.
- [17] T. Salimans and D. A. Knowles. Fixed-form variational posterior approximation through stochastic linear regression. *Bayesian Analysis*, 8(4):837–882, 2013.
- [18] K. Sheppard. Arch, 2014. URL <https://github.com/bashtage/arch>. Python package version 4.3.1.
- [19] M. van der Wilk, A. G. Wilson, and C. E. Rasmussen. Variational inference for latent variable modelling of correlation structure. In *NIPS 2014 Workshop on Advances in Variational Inference*, 2014.
- [20] A. G. Wilson and Z. Ghahramani. Generalised Wishart processes. In *UAI*, 2010.
- [21] Y. Wu, J. M. Hernández-Lobato, and Z. Ghahramani. Dynamic covariance models for multivariate financial time series. In *ICML*, 2013.
- [22] Y. Wu, J. M. Hernández-Lobato, and Z. Ghahramani. Gaussian process volatility model. In *NIPS*, 2014.